

**FABRICATION OF POROUS CARBONATED
HYDROXYAPATITE BY A SPONGE TEMPLATE
AND CARBONATION TECHNIQUE**

SUNARSO

UNIVERSITI SAINS MALAYSIA

2012

**FABRICATION OF POROUS CARBONATED
HYDROXYAPATITE BY A SPONGE TEMPLATE AND
CARBONATION TECHNIQUE**

by

SUNARSO

**Thesis submitted in fulfillment of the requirements
for the degree of
Master of Science**

November 2012

Saya isytiharkan bahawa kandungan yang dibentangkan di dalam tesis ini adalah hasil kerja saya sendiri dan telah dijalankan di Universiti Sains Malaysia kecuali dimaklumkan sebaliknya. Tesis ini juga tidak pernah disertakan untuk ijazah yang lain sebelum ini.

Disaksikan Oleh:

.....

Tandatangan Calon

Nama Calon: Sunarso

.....

Tandatangan Penyelia/Dekan

ACKNOWLEDGEMENTS

I cherish this chance to show my sincere gratefulness to my supervisor, Prof. Ahmad Fauzi Mohd Noor and co-supervisor Dr. Shah Rizal Kasim for their support, inspiration and guidance to complete this research project at USM. I would like to thank Prof. Radzali Othman for his advices, help and guidance. I would also like to acknowledge Dr. Ika Dewi Ana at Universitas Gadjah Mada and Prof. Kunio Ishikawa at Kyushu University, for their valuable support and advices.

I am grateful to JICA-AUN/SEED-Net program for financial support and opportunity to undertake this work. Thank you very much to AUN/SEED-Net Chief Advisor, Prof. Miki Chitoshi, Ms. Kanchana Patanasakdikul, Ms. Siriporn Rungrueangtanya, Ms. Karnkitti Patanasuthikul, and Mrs. Irda and Mrs. Norpisah from USM.

I would like to thank all lecturers, administrative and technical staffs in the School of Materials and Mineral Resources Engineering, USM, for their assistance and support. I also want to express my gratitude to all postgraduate students in School of Materials and Mineral Resources Engineering, USM, especially, Umar Al-Amani Azlan, Nor Nazida Awang, Mohd Hasmizam Razali, Yanny Marlina Baba Ismail, Kee Chia Ching, Nilar Lwin, and all friends from the same research group.

Finally, I would like to take this opportunity to express my gratitude to my parents for their love, advice and support. Special thanks to my beloved one, Azizah Intan Pangesty for her endless care, support and encouragement.

TABLES OF CONTENTS

	Page
ACKNOWLEDGEMENTS	ii
TABLE OF CONTENTS	iii
LIST OF TABLES	vii
LIST OF FIGURES	ix
LIST OF ABBREVIATIONS	xiv
LIST OF SYMBOLS	xv
LIST OF PUBLICATIONS	xvi
ABSTRAK	xvii
ABSTRACT	xviii
CHAPTER 1: INTRODUCTION	
1.1 Introduction	1
1.2 Problem Statement	2
1.3 Objectives of the Research	5
1.4 Research Approach	5
CHAPTER 2: LITERATURE REVIEW	
2.1 Tissue Engineering and Biomaterials	9
2.1.1 Tissue Engineering	9
2.1.2 Biomaterials for Bone	11
2.2 Apatite Biomaterials	14
2.2.1 Hydroxyapatite	14
2.2.2 Substituted Hydroxyapatite	15
2.3 Carbonated Hydroxyapatite	16
2.3.1 General Overview	16

2.3.2	Carbonated Hydroxyapatite As Bone Substitute	17
2.4	Porous Carbonated Hydroxyapatite As Ideal Bone Substitute	18
2.5	Sponge Template Method for Fabricating Porous Apatite Biomaterials	19
2.6	Porous Apatite Biomaterials from Nano-sized Hydroxyapatite Powders	22
2.7	Methods for Synthesis Nano-sized Hydroxyapatite Powders	23
2.7.1	Hydrothermal Treatment	23
2.7.2	Nanoemulsion Method	25
2.8	Carbonation of Hydroxyapatite using Wet Carbon Dioxide Gas	26
2.9	Sintering and Sintering Additives for Porous Apatite Biomaterials	26
2.9.1	Sintering for Fabricating Porous Apatite Biomaterials by Sponge Template	26
2.9.2	Sintering Additives for Porous Apatite Biomaterials	28
2.10	Bioactivity Evaluation	28
 CHAPTER 3: MATERIALS AND METHODOLOGY		
3.1	Introduction	31
3.2	Part I (Porous C-HAP from Micron-sized Commercial HAP Powders)	31
3.2.1	Preparation of Porous HAP	32
3.2.2	Carbonation of Sintered Porous HAP	34
3.2.3	Effect of $\text{Mg}(\text{NO}_3)_2$ Addition	36
3.3	Part II (Porous C-HAP from Nano-sized HAP Powders)	37
3.3.1	Hydrothermal Treatment	38
3.3.1.1	Preparation of Hydrothermal-derived HAP Powders	38
3.3.1.2	Preparation of Porous C-HAP from Hydrothermal-derived HAP Powders	39

3.3.2	Nanoemulsion Method	40
3.3.2.1	Preparation of Nanoemulsion-derived HAP Powders	40
3.3.2.2	Preparation of Porous C-HAP from Nanoemulsion-derived HAP Powders	42
3.4	Part III (Bioactivity Evaluation)	43
3.5	Characterizations	45
3.5.1	X-Ray Diffraction (XRD)	46
3.5.2	Fourier Transform Infra-Red (FTIR) Spectroscopy	46
3.5.3	Carbon Hydrogen Nitrogen (CHN) Analyzer	47
3.5.4	Energy Dispersive X-Ray (EDX)	47
3.5.5	Optical Microscope (OM)	47
3.5.6	Field Emission Scanning Electron Microscope (FESEM) and Scanning Electron Microscope (SEM)	48
3.5.7	Transmission Electron Microscope (TEM)	48
3.5.8	Viscosity Measurement	49
3.5.9	Density and Porosity Measurement	49
3.5.10	Compressive Strength	50
 CHAPTER 4: RESULTS AND DISCUSSION		
4.1	Introduction	52
4.2	Part I (Porous C-HAP from Micron-sized Commercial HAP Powders)	52
4.2.1	Preparation of Porous HAP	53
4.2.2	Carbonation of Sintered Porous HAP	66
4.2.2.1	Effect of Cooling Temperatures	66
4.2.2.2	Effect of Flow Times	75

4.2.2.3	Morphology of Porous C-HAP	78
4.2.2.4	Physical Properties of Porous C-HAP	79
4.2.3	Effect of $\text{Mg}(\text{NO}_3)_2$ Addition	81
4.3	Part II (Porous C-HAP from Nano-sized HAP Powders)	87
4.3.1	Porous C-HAP from Hydrothermal-derived HAP Powders	88
4.3.1.1	Characterization of Synthesized Powder	89
4.3.1.2	Preparation of Porous CH-1	92
4.3.2	Porous C-HAP from Nanoemulsion-derived HAP Powders	96
4.3.2.1	Characterization of Synthesized Powders	96
4.3.2.2	Preparation of Porous CN-1	99
4.3.2.3	Comparison between Porous C-1 and CN-1	103
4.4	Part III (Bioactivity Evaluation)	106
CHAPTER 5: CONCLUSION AND RECOMMENDATION		
5.1	Conclusions	117
5.2	Recommendations for Future Research	119
REFERENCES		120
APPENDICES		129
APPENDIX A		130
APPENDIX B		133

LIST OF TABLES

2.1	Optimal pores for bone tissue formation	14
2.2	Models for Ca-defHAP formula	15
2.3	Component of Adult Human Bone	18
2.4	Characteristic of hydrothermal powder and ideal powder	24
3.1	Liquid to Powder Ratio	33
3.2	Codes of carbonated porous specimens	35
3.3	The amount of $Mg(NO_3)_2$ added to HAP slurry	37
3.4	Ion concentration of SBF and human blood plasma	44
3.5	Reagents for preparation of 1000mL SBF	45
4.1	(002) position, lattice parameter, CO_3^{2-} content and c/a ratio, of porous HAP and porous C-HAP in powdered form (flow time: 20min)	69
4.2	(002) position, lattice parameter, CO_3^{2-} content and c/a ratio, of porous HAP and porous C-HAP in powdered form (flow time: 40min)	69
4.3	(002) position, lattice parameter, CO_3^{2-} content and c/a ratio, of porous HAP and porous C-HAP in powdered form (flow time: 60min)	70
4.4	CO_3^{2-} peaks observed from porous C-HAP	74
4.5	(002) position, lattice parameter, CO_3^{2-} content and a/c ratio, of porous HAP and porous C-HAP in powdered form (cooling temperature: 200°C)	77
4.6	(002) position, lattice parameter, CO_3^{2-} content and a/c ratio, of porous HAP and porous C-HAP in powdered form (cooling temperature: 300°C)	77
4.7	(002) position, lattice parameter, CO_3^{2-} content and a/c ratio, of porous HAP and porous C-HAP in powdered form (cooling temperature: 400°C)	78
4.8	The pH of solution and phase compositions of the synthesized powder after hydrothermal method	90

4.9	CO_3^{2-} content, crystallite size and lattice parameter of as-synthesized HAP powders	97
4.10	The CO_3^{2-} absorption peaks observed in as-synthesized HAP powders, HN-1 and CN-1 (in powdered form)	101
A1	Chemical formula, moles, mass, molecular weight, volume of starting raw material for nanoemulsion method	131
A2	Dry weight (D), saturated weight (W) and suspended weight (S) obtained by Archimedes method	131
A3	Weight percent of calcium (Ca) and phosphorus (P) obtained from EDX	132

LIST OF FIGURES

1.1	Flowchart for fabrication of porous C-HAP from micron-sized HAP powders (Part I)	6
1.2	Flowchart for fabrication of porous C-HAP from nano-sized HAP powders (Part II)	7
1.3	Flowchart for bioactivity evaluation	8
2.1	Approaches in tissue engineering	10
2.2	Processing route to produce macroporous ceramics	20
2.3	SEM image after PU had been removed	21
2.4	Schematic illustration of the PU foam removal mechanism	21
2.5	Comparison of SEM images of the surface of scaffolds fabricated using HAP coarse particles (left) and HA nanoparticles (right)	23
2.6	Influence of sintering temperature on microporosity. A: Sharp decrease of microporosity (0.1-10nm) with sintering temperature and no change of macroporosity. B: Decrease of osteoinductive potentials with sintering temperature	27
2.7	Porous α -TCP after immersion in SBF solution for 0, 1, 3 and 7 days	29
2.8	Schematic presentations of the origin of the negative charge on the HA surface (in case of the (100) projection of crystal structure), and the process of bone-like apatite formation thereon in SBF	30
3.1	Flowchart of porous C-HAP preparation	33
3.2	Sintering profile used to fabricate porous C-HAP from micron-sized HAP powders	34
3.3	Sintered porous HAP 3.0	34

3.4	Schematic of Carbonation	35
3.5	Flowchart for preparing HAP+Mg(NO ₃) ₂ slurry	37
3.6	Flowchart for synthesis of HAP powders by hydrothermal treatment	39
3.7	Flowchart for synthesis of HAP powders by nanoemulsion method	41
3.8	Sintering profile used to fabricate porous C-HAP from nano-sized HAP powders	43
3.9	Schematic illustration of the density and porosity measurement by archimedes method	50
3.10	Schematic illustration for compressive strength measurement	51
4.1	SEM images of commercial HAP powders at (A) 10K and (B) 30K magnifications	53
4.2	TEM image of commercial HAP powders	53
4.3	SEM image of sponge template	54
4.4	Viscosity of the slurries versus H ₂ O/HAP ratio	55
4.5	XRD patterns of sintered HAP powders	57
4.6	FTIR analysis of sintered HAP powders	57
4.7	Optical micrograph of porous HAP: (A) HAP 2.5, (B) HAP 3.0, and (C) HAP 3.5 (yellow arrows: clogged pores)	59
4.8	SEM images of sintered porous HAP: HAP 2.5 (A), HAP 3.0 (B), and HAP 3.5 (C). Yellow and red arrow are the HAP clogged pores and strut replication	60
4.9	Micropores of sintered porous HAP 2.5 (A&B), HAP 3.0 (C&D), and HAP 3.5 (E&F)	61
4.10	(A) hollow struts (yellow arrows) and interconnected holes (red arrows) and (B) cross section of hollow strut observed in sponge template method	62

4.11 The apparent porosity of porous HAP as a function of H ₂ O/HAP ratio	63
4.12 The bulk density of porous HAP as a function of H ₂ O/HAP ratio	64
4.13 Compressive strength of porous HAP against H ₂ O/HAP ratio	65
4.14 X-Ray diffraction patterns of porous HAP and C-HAP in powdered form (flow time: 20min)	67
4.15 X-Ray diffraction patterns of porous HAP and C-HAP in powdered form (flow time: 40min)	68
4.16 X-Ray diffraction patterns of porous HAP and C-HAP in powdered form (flow time: 60min)	68
4.17 Carbonate content with respect of cooling temperatures	72
4.18 FTIR spectra of porous C-HAP in powdered form at different cooling temperatures: (A) flow time: 20min, (B)flow time: 40min, and (C) flow time: 60min	73
4.19 XRD patterns of porous HAP and C-HAP in powdered form (cooling temperature: 200°C)	75
4.20 XRD patterns of porous HAP and C-HAP in powdered form (cooling temperature: 300°C)	76
4.21 XRD patterns of porous HAP and C-HAP in powdered form (cooling temperature: 400°C)	76
4.22 SEM images of porous HAP (A and B) and C-HAP 200/60 (C and D)	79
4.23 Apparent porosity and bulk density of HAP 3.0 and C-HAP 200/60	80
4.24 Compressive strength of HAP 3.0 and C-HAP 200/60	80
4.25 XRD patterns of C-HAP 200/60 (C-0) and C-HAP 200/60 with MgO addition (C-1 to C7) in powdered form	83
4.26 Compressive strength of C-HAP 200/60 and C-HAP 200/60 with MgO	83

addition	
4.27 SEM images of C-HAP 200/60: without MgO (A), 1wt% MgO (B), 3wt% MgO (C), 5wt% MgO (D), and 7wt% MgO (E)	85
4.28 Apparent porosity (A) and bulk density of porous C-HAP with MgO addition (B)	86
4.29 Carbonate content of C-HAP 200/60 with MgO addition	87
4.30 XRD patterns of β -TCP powders before and after hydrothermal method at different times	89
4.31 SEM images of the β -TCP powders (A) and powders obtained by hydrothermal treatment of β -TCP for 72h (B)	91
4.32 TEM images of β -TCP particles (A) and as-synthesized particles: biphasic particle (B), HAP single particle (C and D)	92
4.33 XRD patterns of as-synthesized HAP powders obtained after hydrothermal method of β -TCP for 72h and porous CH-1 (in powdered form) after sintering at 900°C	93
4.34 Phase composition of as-synthesized powders obtained from hydrothermal method of β -TCP for 72h and porous CH-1 calculated from XRD pattern by Expert High Score Software	94
4.35 SEM images of porous biphasic β -TCP/HAP obtained from hydrothermal powders after sintering at 900°C: (A) 60X, (B) 5000X	95
4.36 XRD pattern of as-synthesized HAP powders obtained from nanoemulsion method	97
4.37 FTIR spectra of as-synthesized HAP powders obtained from nanoemulsion method	98
4.38 TEM images of commercial HAP (A) and as-synthesized HAP obtained by	99

the nanoemulsion method (B)	
4.39 XRD patterns of as-synthesized HAP obtained from nanoemulsion and porous CN-1 (in powdered form)	100
4.40 FTIR spectra of as-synthesized HAP powders obtained from nanoemulsion, porous HN-1 and CN-1 (in powdered form)	101
4.41 Comparison between CO_3^{2-} content of HN-1 and CN-1	102
4.42 SEM images of porous CN-1	103
4.43 CO_3^{2-} content of porous C-1 and CN-1	104
4.44 Porous structure of C-1 (A) and CN-1 (B) and overall microstructure of C-1 (C) and CN-1 (D)	105
4.45 Comparison between compressive strength of porous C-1 and CN-1	105
4.46 SEM images of porous HAP 3.0 (A&B), porous C-1 (C&D), and porous CN-1 (E&F) after immersion in SBF solution for 1 week at $36.5 \pm 1.0^\circ\text{C}$	108
4.47 SEM images of porous HAP 3.0 (A&B), porous C-1 (C&D), and porous CN-1 (E&F) after immersion in SBF solution for 2 weeks at $36.5 \pm 1.0^\circ\text{C}$	109
4.48 SEM images of porous HAP 3.0 (A&B), porous C-1 (C&D), and porous CN-1 (E&F) after immersion in SBF solution for 4 weeks at $36.5 \pm 1.0^\circ\text{C}$	111
4.49 SEM images, EDX spectra and Ca/P molar ratio of granule-like morphology on porous CN-1 surface (A), salt on porous CN-1 surface (B) and porous C-1 (C) after soaking in SBF solution for 2 weeks at $36.5 \pm 1.0^\circ\text{C}$	112
4.50 EDX spectra and Ca/P molar ratio of porous HAP 3.0 (A), porous C-1 (B), and porous CN-1 (C) after immersion in SBF solution for 4 weeks at $36.5 \pm 1.0^\circ\text{C}$	114

LIST OF ABBREVIATIONS

HAP	Hydroxyapatite
C-HAP	Carbonated Hydroxyapatite
α -TCP	Alpha Tricalcium Phosphate
β -TCP	Beta Tricalcium Phosphate
kPa	Kilopascal
SBF	Simulated Body Fluid
SEM	Scanning Electron Microcopy
FESEM	Field Emission Scanning Electron Microscopy
TEM	Transmission Electron Microscopy
PU	Polyurethane
XRD	X-Ray Diffraction
FTIR	Fourier Transform Infra-Red
CHN	Carbon Hydrogen Nitrogen
XRF	X-Ray Fluorescence
EDX	Energy Dispersive X-Ray

LIST OF SYMBOLS

α	Alpha
β	Beta
θ	Theta
$^{\circ}$	Degree
μm	Micrometer
nm	Nanometer
P	Poise
\AA	Angstrom
A_r	Atomic weight
M_r	Molecular weight

LIST OF PUBLICATIONS

Proceeding:

1. Sunarso, Ahmad Fauzi, M. N., Kasim, S. R., Radzali, O., Ana, I.D., Ishikawa, K. (2011), Fabrication of Interconnected Porous Hydroxyapatite, *Science and Technology Community Development 2011 & International Symposium on Material Science Engineering and Energy Technology (STCD 2011)*, Faculty of Science and Technology, Thammasat University, Bangkok, Thailand 30th June – 1st July 2011.
2. Sunarso, Ahmad Fauzi, M. N., Kasim, S. R., Radzali, O., Ana, I.D., Ishikawa, K. (2011), Wet CO₂ Gas As A Carbonate Source On Fabrication Of Interconnected Porous Carbonated Hydroxyapatite, *The 11th Asian BioCeramics Symposium, National Institute of Materials Science (NIMS), Sengen Site, Tsukuba, Ibaraki, Japan 30th November – 2nd December 2011*.
(Awarded as the most outstanding presentation)
3. Sunarso, Ahmad Fauzi, M. N., Kasim, S. R., Radzali, O., Ana, I.D., Ishikawa, K. (2012), Synthesis of Ca-deficient Carbonated Hydroxyapatite Nanoparticle, *International Conference on X-Rays & Related Techniques in research & Industry, Vistana Hotel, Penang, Malaysia, 3rd-5th July 2012*

FABRIKASI HIDROKSIAPATIT TERKARBONAT BERLIANG MELALUI KAEDAH TEMPLAT SPAN DAN PENGKARBONATAN

ABSTRAK

Hidroksiapatit terkarbonat berliang (C-HAP) telah berjaya dihasilkan melalui teknik templat span dan pengkarbonatan daripada hidroksiapatit komersial bersaiz mikron dan hidroksiapatit bersaiz nano (hasil sintesis). Pengkarbonatan terhadap hidroksiapatit berliang tersinter di dalam gas CO_2 basah sewaktu penyejukan, telah berjaya menggabungkan ion CO_3^{2-} ke dalam HAP berliang. Proses pengkarbonatan dilakukan pada tiga suhu penyejukan (200, 300 dan 400°C) dan tiga masa aliran gas (20, 40 dan 60 minit). Keadaan optimum untuk pengkarbonatan diperolehi selepas gas dialirkan pada suhu penyejukan 200°C selama 60 minit. Peningkatan suhu penyejukan menyebabkan penurunan kandungan ion CO_3^{2-} manakala peningkatan masa aliran gas menyebabkan peningkatan kandungan ion CO_3^{2-} . Penambahan $\text{Mg}(\text{NO}_3)_2$ yang setara dengan 1, 3, 5 dan 7% MgO (%berat) dilakukan untuk meningkatkan kekuatan mekanikal C-HAP berliang. Kekuatan mampatan C-HAP berliang mencapai nilai tertinggi selepas penambahan $\text{Mg}(\text{NO}_3)_2$ yang setara dengan 1% MgO. C-HAP berliang yang difabrikasi daripada serbuk HAP yang diperolehi melalui kaedah nanoemulsi mempunyai kandungan ion CO_3^{2-} lebih tinggi (1.70%) berbanding C-HAP berliang yang difabrikasi daripada serbuk HAP komersial bersaiz mikron (1.25%). Ianya menunjukkan bahawa saiz partikel yang lebih kecil meningkatkan kereaktifan spesimen berliang terhadap gas CO_2 semasa pengkarbonatan. Selepas perendaman dalam larutan SBF selama 1, 2 dan 4 minggu pada suhu $36.5 \pm 1.0^\circ\text{C}$, lapisan bak apatit berkembang lebih cepat pada C-HAP berliang yang mempunyai kandungan ion CO_3^{2-} lebih tinggi ini mencadangkan bahawa teknik pengkarbonatan yang digunakan dalam kajian ini berupaya untuk meningkatkan bioaktiviti produk berliang.

FABRICATION OF POROUS CARBONATED HYDROXYAPATITE BY A SPONGE TEMPLATE AND CARBONATION TECHNIQUE

ABSTRACT

Porous carbonated hydroxyapatite (C-HAP) was successfully fabricated by a sponge template and carbonation technique from micron-sized commercial HAP powders and synthesized nano-sized HAP powders. The carbonation of the porous HAP, performed during the cooling stage of the sintering process under wet carbon dioxide (CO_2) gas, was successful in incorporating CO_3^{2-} ions into porous HAP. Carbonation was carried out at three different cooling temperatures (200, 300 and 400°C) and flow times (20, 40 and 60min). The optimum condition for carbonation in terms of CO_3^{2-} content was obtained after the gas had been passed through at a cooling temperature of 200°C for 60min. It was found that an increase in cooling temperature resulted in a decrease in CO_3^{2-} ion content, whilst a longer flow time yielded in an increase of CO_3^{2-} ion content. $\text{Mg}(\text{NO}_3)_2$, which was equivalent to 1, 3, 5 and 7 wt% of MgO, was added to enhance the mechanical strength of porous C-HAP. The compressive strength of porous C-HAP reached the highest value after an addition of $\text{Mg}(\text{NO}_3)_2$ equivalent to 1 wt% of MgO. It was observed that the porous C-HAP fabricated from nanoemulsion-derived HAP powders possessed a higher CO_3^{2-} ion content (1.70 wt%) compared to that of porous C-HAP fabricated from micron-sized commercial HAP powders (1.25 wt%), indicating that the smaller particle size of the starting material might have enhanced the reactivity of the porous specimens to CO_2 gas during carbonation. After immersion in SBF solution for 1, 2 and 4 weeks at $36.5 \pm 1.0^\circ\text{C}$, apatite-like layer grew faster in the porous C-HAP with higher CO_3^{2-} ion content, suggesting that the carbonation technique used in this study was able to enhance the bioactivity performance of the porous product.

CHAPTER 1

INTRODUCTION

1.1 Introduction

Conventionally, autograft (bone harvested from another site from the same patient) is the gold standard for bone substitution procedure since it provides essential osteoinductive factors required for bone healing (Burg et al., 2000; Salgado et al., 2004). However, the use of this standard is restricted due to the limitation of donor site. Allograft (bone taken from other patients) is an alternative to the usage of autograft. Allograft also suffers from some drawbacks, such as the potential of immune rejection and disease transmission (Salgado et al., 2004).

An alternative material, which fulfills the requirements for being used as bone substitute, in abundant amount is therefore required. The ideal bone substituting material should have the properties that are close to those of natural bone. Bone has a porous structure that provides space for tissue ingrowth during the bone repairing process. Besides, bone is also composed of an inorganic component that is usually simplified as hydroxyapatite, formulated by $\text{Ca}_{10}(\text{PO}_4)_6(\text{OH})_2$. In fact, hydroxyapatite in natural bone contains some impurities, mainly carbonate ions (CO_3^{2-}), and is thus more accurately called carbonated hydroxyapatite (Habibovic et al. 2010).

Many efforts were developed to fabricate porous synthetic materials from HAP (Li et al., 2002; Munar et al., 2006; Jun et al., 2007; Jo et al., 2009) which is considered the ideal bone substitute material due to its similarity with bone

(Yoshikawa and Myoui, 2005). Moreover, porous HAP which possesses interconnected pores exhibited excellent bone ingrowth (Yoshikawa et al., 2009). Several methods are available to fabricate porous HAP, such as gel casting, slurry foaming and sponge template methods (Swain, 2009). Among them, the sponge template method is considered as the first and the most popular technique used to fabricate porous ceramics due to its simplicity and the excellent result on interconnectivity required as an ideal bone substitute (Studart et al., 2006).

Porous HAP has been accepted to be able to promote bone tissue formation (Munar, 2006). However, HAP was not resorbed with osteoclasts (bone resorbing cells) and hence would not be replaced with new bone (Maruta et al., 2011). The ability of a material to be resorbed by osteoclast is believed to be related to the solubility of bone substitute material (Ito et al., 1997). Accordingly, the incorporation of one CO_3^{2-} ion per unit cell in HAP increased the solubility product significantly. Moreover, CO_3^{2-} ion is the main impurity found in human bone mineral (Habibovic et al., 2010). Therefore, the drawback of the porous HAP application in bone substitute can be overcome by incorporating carbonate (CO_3^{2-}) ions to the crystal structure to form carbonated hydroxyapatite. Porous material from carbonated hydroxyapatite (C-HAP) thus becomes an ideal material for bone substitute.

1.2 Problem Statement

Despite being considered as an ideal material for bone substitute, there are only limited papers reported on the fabrication of porous C-HAP (Lee et al., 2008; Wakae et al., 2008; Maruta et al., 2011). Those researchers had successfully fabricated porous C-HAP by using salt leaching and sponge template. Wakae et al. (2008) had fabricated porous C-HAP by using α -tricalcium phosphate (α -TCP) as a

precursor. Sponge template was used to prepare a porous α -TCP. Initially, the porous α -TCP was prepared by dipping the α -TCP slurry using a sponge template, followed by sintering to burn out the template and densify the porous ceramics. Sintered porous α -TCP was then transformed to C-HAP by hydrothermal treatment in a phosphate solution. Maruta et al. (2011) used calcium hydroxide ($\text{Ca}(\text{OH})_2$) as the precursor to fabricate porous C-HAP by the sponge template method. Initially, $\text{Ca}(\text{OH})_2$ slurry was coated onto a polyurethane foam. Subsequently, the coated foam was sintered in carbon dioxide (CO_2) and oxygen (O_2) atmosphere to produce porous CaCO_3 . Sintered porous CaCO_3 was then transformed to porous C-HAP by immersing it in a phosphate solution at 60°C for two weeks. Both of the papers (Maruta et al., 2011 and Wakae et al., 2008) had used the dissolution-precipitation reaction to transform the precursors to C-HAP phase. Moreover, the mechanical strengths of all porous C-HAP fabricated by these methods were relatively low (5-25 kPa). Therefore, it is necessary to develop an alternative way to fabricate porous C-HAP.

In this study, a new approach to fabricate porous sintered C-HAP by a sponge template was introduced as an alternative to the present available techniques. In this approach, porous C-HAP was fabricated using HAP powder as the starting material followed by carbonation after sintering. Carbonation was applied using a technique whereby the sample was cooled down during the sintering stage under wet CO_2 gas, which was developed from Yanny-Marliana (2011). The carbonation was performed by flowing wet CO_2 gas at a cooling temperature of 200°C for 20min. However the carbonation process in the present study was carried out with additional parameters to study the effect of those parameters on CO_3^{2-} content of the carbonated products. The additional parameters investigated in this study were the cooling temperatures,

during which wet CO₂ gas was flowed in, and this was varied at 200, 300 and 400°C, and the flowing gas times or duration (20, 40 and 60min).

Since the mechanical strength of porous product is very low, a biocompatible sintering aid is thus required to enhance the mechanical strength of the porous C-HAP. Magnesium oxide (MgO) is a biocompatible sintering aid with no cytotoxicity after being implanted in living tissue in vivo (Ryu et al., 2004). MgO, therefore, is an ideal sintering aid for porous C-HAP. However, the usage of MgO powder directly in the slurry is not suitable, due to the difficulty in obtaining homogenous mixture since, it is insoluble in water (Lindberg et al., 1990). Hence highly soluble compounds are the ideal candidates for this purpose.

In this study, magnesium nitrate (Mg(NO₃)₂) was used to produce MgO as the sintering aid to enhance the mechanical strength of porous C-HAP. Mg(NO₃)₂ was used instead of MgO since it is a highly soluble compound in a water solvent and had been proved to be homogeneously distributed (Huang et al., 2003). Huang et al. (2003) added 3, 6 and 9 wt% of Mg(NO₃)₂ to a silicon carbide ceramic. However, in this study, the amount of sintering aid was calculated from the MgO as the decomposed compound. The calculated amount of MgO investigated in this study were 1, 3, 5, 7 wt%.

Nano-sized HAP powders possess larger surface area as compared to the micron-sized commercial HAP powders. Hypothetically, larger surface area will increase the reactivity of the nano-sized HAP powders to react with wet CO₂ gas. The use of micron-sized commercial HAP powders as the starting material to fabricate porous C-HAP may result in low CO₃²⁻ content. Therefore, in this research,

nano-sized HAP powders were also used and investigated as the starting material for the fabrication of porous C-HAP.

Animal experiment is usually conducted to evaluate the bioactivity performance of bone substituting materials. However, it has been reported that simulated body fluid (SBF) is able to predict the bioactivity of bone substitute material without using animal experiment (Kokubo and Takadama, 2006). Therefore, in this study, SBF will be used to evaluate the bioactivity performance of porous C-HAP.

1.3 Objectives of the Research

The objectives of this research were:

1. Preparation of porous sintered C-HAP fabricated from micron-sized commercial HAP powders and nano-sized HAP powders by the sponge template and carbonation technique.
2. Investigation of the effect of MgO content (1, 3, 5, and 7 wt%), obtained from the decomposition of $\text{Mg}(\text{NO}_3)_2$ addition, on the mechanical strength of porous sintered C-HAP.
3. Evaluation of the bioactivity of, as-fabricated porous C-HAP, using simulated body fluid (SBF).

1.4 Research Approach

In this study the experiment was divided into three parts. In the first part, porous HAP was fabricated using micron-sized commercial HAP powders followed by carbonation to produce porous C-HAP. $\text{Mg}(\text{NO}_3)_2$ was added as sintering aid to enhance the mechanical strength of porous C-HAP.

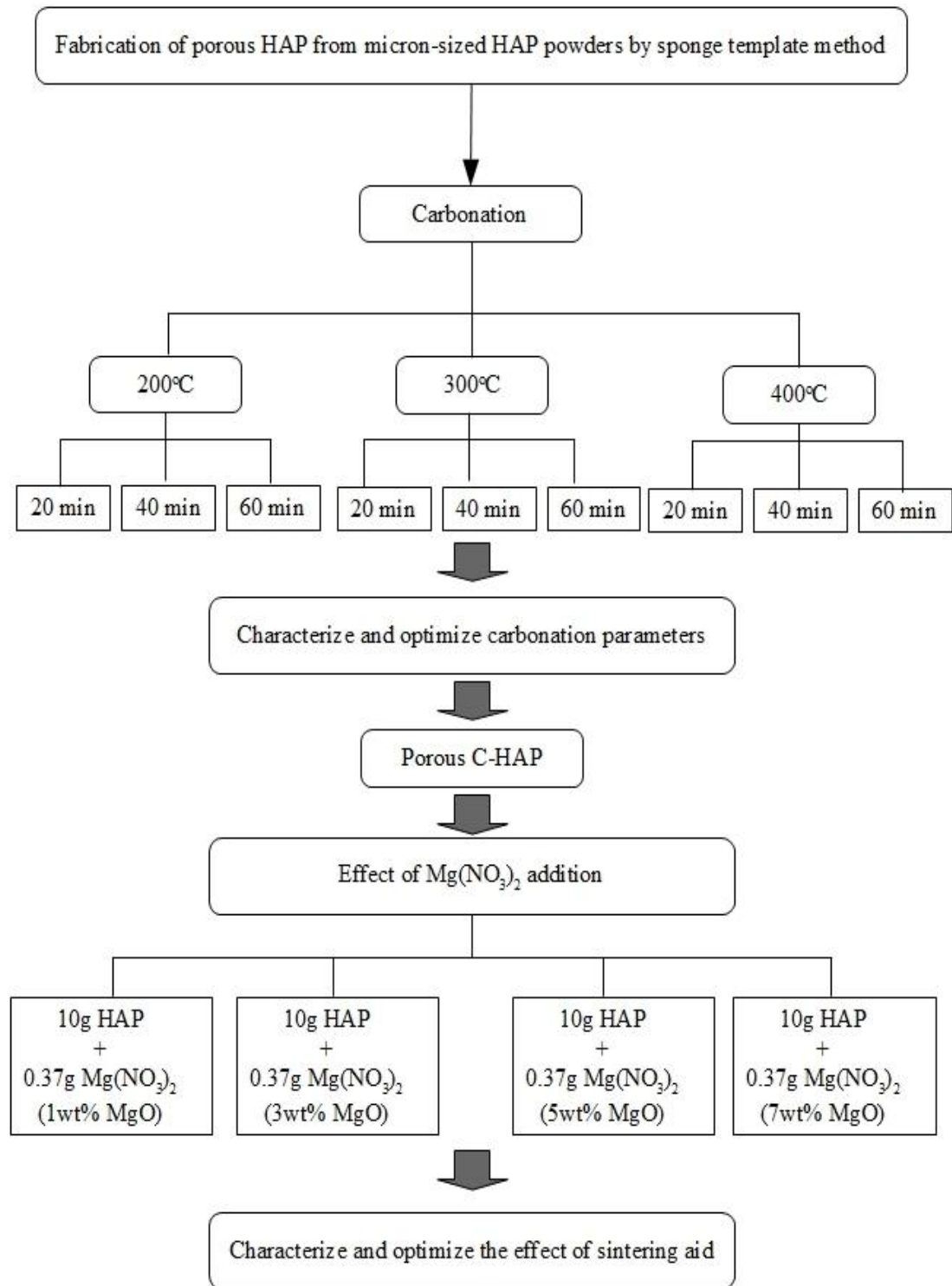


Fig. 1.1 Flowchart for the fabrication of porous C-HAP from micron-sized HAP powders (Part I)

The second part investigated the fabrication of porous C-HAP using nano-sized HAP powders. Firstly, nano-sized HAP powders were synthesized using a hydrothermal method. However, since the hydrothermal method produced only

75.9% HAP, another method was then used to synthesize nano-sized HAP powders, and this was the nanoemulsion method. The optimum parameters for porous C-HAP fabrication obtained from the first part are used in the second part.

The third part was the evaluation of bioactivity performance of the obtained porous C-HAP both from part I and part II. The evaluation was conducted by immersing the porous specimens in SBF solution for 1, 2 and 4 weeks at a temperature of $36.5 \pm 1.0^\circ\text{C}$, which is the temperature of human body. The following flowcharts show the details of the three parts of the experimental working in this research.

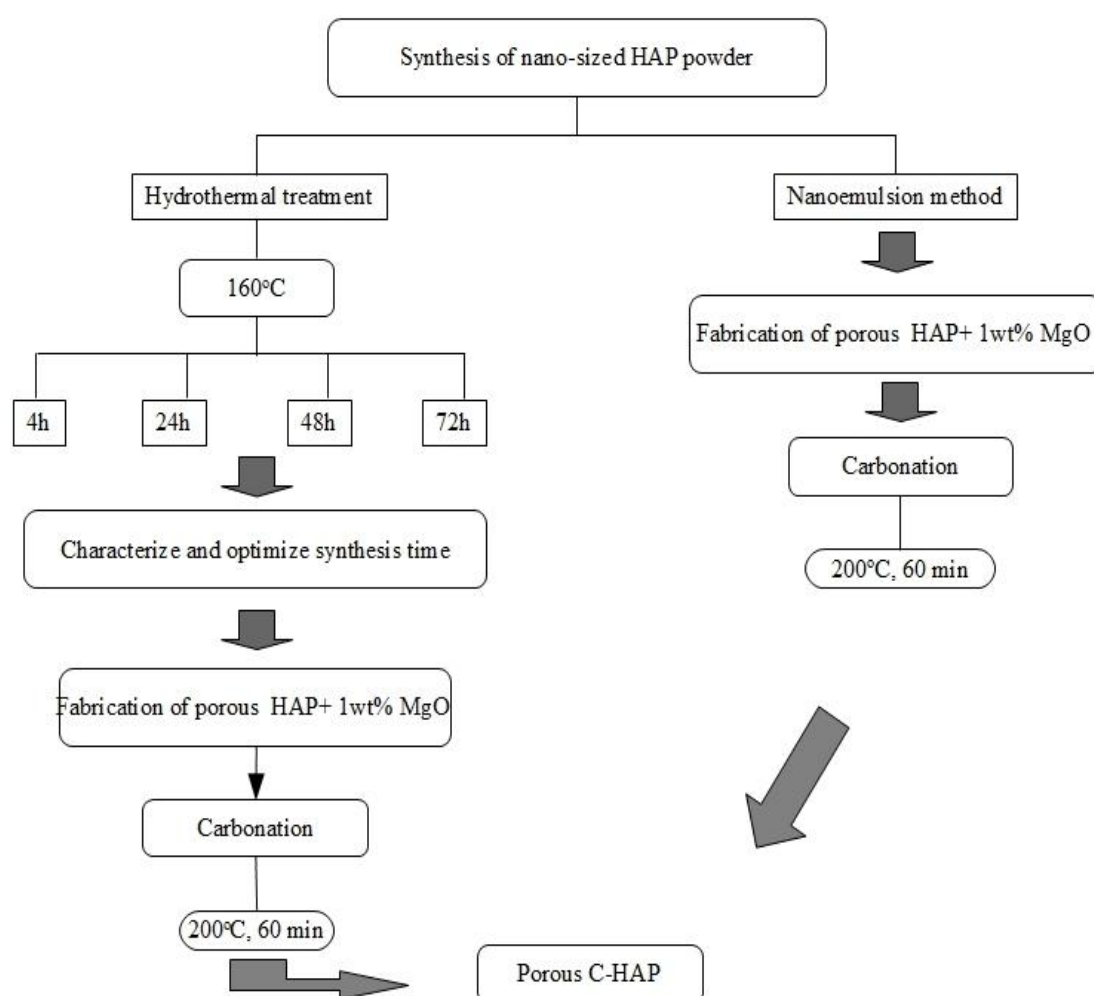


Fig. 1.2 Flowchart for the fabrication of porous C-HAP from nano-sized HAP powders (Part II)

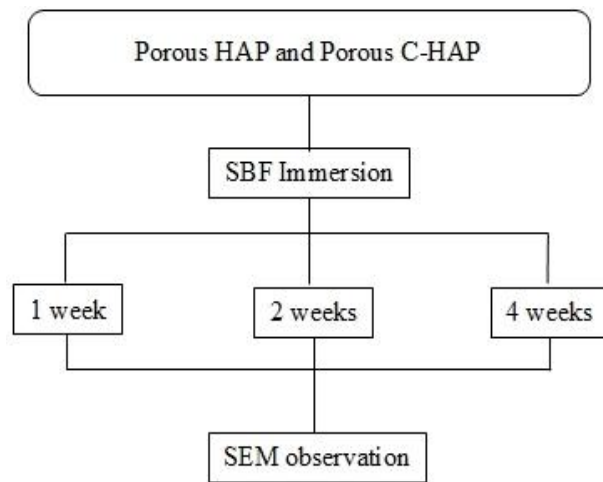


Fig. 1.3 Flowchart for the bioactivity evaluation (Part III)

CHAPTER 2

LITERATURE REVIEW

2.1 Tissue Engineering and Biomaterials

2.1.1 Tissue Engineering

Tissue engineering is now rapidly growing to provide the clinical technology which allows for improvements of human life (Ikada, 2006). The term of “tissue engineering” initially was introduced at the panel meeting in 1987 held by the National Science Foundation (NSF), Boston, USA. However, the actual definition of “tissue engineering” as it is applied today was described by Vacanti and Vacanti (1991). Vacanti and Vacanti (1991) stated that the “tissue engineering” is a scientific discipline dedicated to the generation of new tissue using the principles of engineering in combination with an understanding and application of the biologic sciences. Furthermore, Ikada (2006) added that there are three principles in tissue engineering i.e. cells, scaffold, and growth factors. In case of bone tissue, it has been studied that there are two kinds of cells that are involved in bone remodeling process where old tissue is replaced by new tissue i.e. osteoclasts (bone resorbing cells) and osteoblasts (bone depositing cells) (Phan et al., 2004).

The second principle of tissue engineering is a template (natural or synthetic) where a new tissue is formed or so called scaffold material, which according to Vacanti and Vacanti (1991), should be biodegradable (able to being break down in the body), bioresorbable (resorb by osteoclasts) and three dimensional porous structure to provide space for new bone formation as well as penetration of new

formed tissue. The third principle of tissue engineering, which is occasionally added, is growth factors. In bone tissue engineering, growth factors are small proteins that are able to induce new bone tissue formation (Tielinen, 2003).

Gomes (2004) stated that basically, there are two approaches in bone tissue engineering: (A) acellular scaffold and (B) cell-seeded scaffold as illustrated in Fig. 2.1. In acellular approach, the scaffold is implanted to induce tissue ingrowth by interaction with surrounding tissue. The success of this approach depends on the infiltration of cells from the living tissue to organize and at the end to repair the lost tissue. In the second approach, scaffold provides an adhesive substrate and physical support for implanted cells to form new tissue.

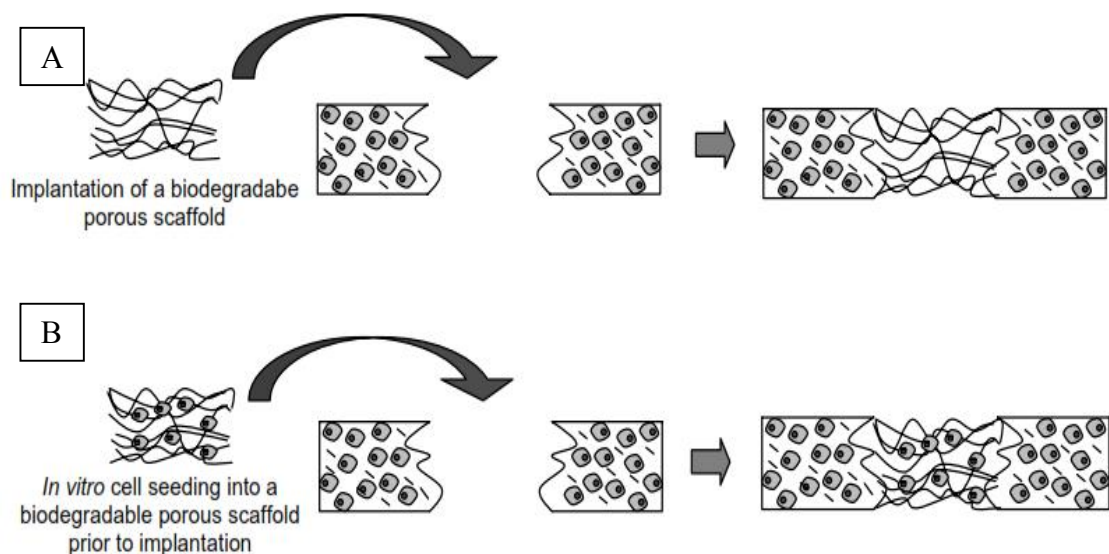


Fig. 2.1 Approaches in tissue engineering (Gomes, 2004)

O'brien (2011) further stated that the term scaffold usually refers to three dimensional biomaterials. Biomaterials therefore, are very critical in tissue engineering.

2.1.2 Biomaterials for Bone

Biomaterials are used as a 3D framework to provide template for cell proliferation to grow a new tissue and also as a delivery device (Ikada, 2006). Biomaterials are defined as materials used to make devices in order to replace a part or a function of the body (Park and Lakes, 2007). Biomaterials application historically can be tracked back from 1860s when Dr. J. Lister developed aseptic surgical technique. Biomaterials could be metals, ceramics, and polymers forms. However, in case of bone substituting materials, ceramics have been widely used due to the close composition with natural bone (Stevens, 2008). According to Albrektsson and Johansson (2001), biomaterials for an ideal bone substitute require some of the following properties:

1. Osteoinductive

Osteoinductive according to Urist (1965) is defined as the ability of materials to induce bone formation in non-bone site (e.g. muscle). In this context, materials are able to stimulate the formation of new bone tissue. One of the widely studied osteoinductive materials is ceramics biomaterials particularly calcium phosphate (CaP) ceramics biomaterials (De Bruijin et al., 2008). De Bruijin et al., (2008) further mentioned that there are some characteristic of calcium phosphate ceramics biomaterials to be osteoconductive. These characteristics are as follows:

- a. Macrostructure

It was reported that bone induction by CaP ceramics biomaterials was never detected on flat CaP ceramics surface. All the osteoinductive CaP ceramics biomaterials possess porous macrostructure. Moreover, it was also reported that bone formation was observed inside the pores of the porous CaP ceramics biomaterials.

b. Microstructure

Beside macrostructure, another element that affects osteoinductive property of CaP ceramics biomaterials is microstructure. It was reported that osteoinduction was increased in the CaP ceramics biomaterials which have higher microporosity (Yuan and Groot, 2005).

c. Chemical composition

Chemical composition also plays an important role in the materials to be osteoinductive. Most of the synthetic biomaterials that demonstrated the ability as osteoinductive biomaterials contain calcium and phosphate ions.

2. Osseointegration

Osseointegration is the ability of a material to bond directly to the living tissue where the material is implanted. Material with osseointegration property usually will form a bone-like layer within the interface of the implant material and living tissue.

3. Osteoconductive

Osteoconductive means that a new bone tissue grows on the surface of the implanted material. An osteoconductive material must allow bone tissue growth on its surface or into its pores or channels. According to Nakamura and Takemoto (2008), there are three important parameters of a material to be osteoconductive. These parameters are as follows:

a. Surface chemistry

It was reported that bioactive CaP ceramics have a high osteoconductivity compared to biologically inert materials such as titanium metals in which the osteoconductivity is limited. Bioactive CaP ceramics biomaterials is defined as the ability of a material to form apatite (bone-like) layer on its surface in the living tissue and then bond to the bone through this layer (Takadama and Kokubo, 2008). Specific surface functional groups were reported to be closely related to this ability. The detail review on bioactivity of biomaterials for bone substitute is presented in section 2.9.

b. Surface topography

Surface topography is also reported to be an important parameter for osteoconductivity of biomaterials. It was reported that on smooth surfaced materials, the orientation of bone cells are random. In vivo study has confirmed that a rough surface may control the tissue formation that lead to the success of bone healing (Anselme, 2000).

c. Porous structure

The third parameter that affects osteoconductivity of biomaterials is the porous structure. It has been reported that biomaterials with a porous structure of adequate pore size and also interconnectivity permit new bone tissue ingrowths and the invasion of blood vessels. Table 2.1 shows the optimum pore size for bone tissue formation.

Table 2.1 Optimal pores for bone tissue formation (Yang et al., 2001)

Reference	Pore size	Porosity	Mineralized tissue ingrowth
Klawitter and Hulbert (1971)	Type I: 2-6 μm	33.5%	No tissue ingrowth.
	Type II: 15-40 μm	46.2%	No bone ingrowth, fibrous tissue ingrowth.
	Type III: 30-100 μm 80% < 100 μm	46.9%	50 μm of bone ingrowth, osteoid and fibrous tissue ingrowth.
	Type IV: 50-100 μm 63% < 100 μm	46.9%	20 μm of bone ingrowth by 11 weeks and 500 μm of ingrowth by 22 weeks, osteoid and fibrous tissue ingrowth.
Whang et al. (1999)	Type V: 60-100 μm 37% < 100 μm	48.0%	600 μm of bone ingrowth by 11 weeks and 1,500 μm of ingrowth by 22 weeks, osteoid and fibrous tissue ingrowth.
	$\leq 100 \mu\text{m}$	35.3%	Not statistically different from untreated controls.
	$\leq 200 \mu\text{m}$	51.0%	Not statistically different from untreated controls.
	$\leq 350 \mu\text{m}$	73.9%	Statistically significant more bone than all other groups.

2.2 Apatite Biomaterials

2.2.1 Hydroxyapatite

Hydroxyapatite (HAP) is “apatite” that refers to $\text{Ca}_{10}(\text{PO}_4)_6(\text{OH})_2$ which is the stoichiometric apatite with Ca/P molar ratio equivalent to 1.67. This HAP is called stoichiometric HAP. In fact, there is the possibility for calcium deficient HAP (Ca-defHAP) to be formed which have Ca/P molar ratio less than 1.67 or more than 1.67 (Elliot, 1994; Zhang and Zhang, 2011). Ca-defHAP is usually obtained by wet chemical synthesis. Several models for Ca-defHAP are presented in Table 2.2.

Table 2.2 Models for Ca-defHAP formula (Elliot, 1994)

1. $\text{Ca}_{10-x}(\text{HPO}_4)_{2x}(\text{PO}_4)_{6-2x}(\text{OH})_2$	$0 \leq x \leq 2$
2. $\text{Ca}_{10-x}(\text{HPO}_4)_x(\text{PO}_4)_{6-x}(\text{OH})_{2-x}$	$0 \leq x \leq 2$
3. $\text{Ca}_{10-x-y}(\text{HPO}_4)_{2x}(\text{PO}_4)_{6-x}(\text{OH})_{2-x-2y}$	$0 \leq x \leq 2$ and $y \leq (1-x/2)$
4. $\text{Ca}_{10-x}(\text{HPO}_4)_x(\text{PO}_4)_{6-x}(\text{OH})_{2-x}$	$0 \leq x \leq 1$
5. $\text{Ca}_{10-x}(\text{HPO}_4)_{2x}(\text{PO}_4)_{6-x}(\text{OH})_{2-x}(\text{H}_2\text{O})_x$	$0 \leq x \leq 1$
6. $\text{Ca}_{9-x}(\text{HPO}_4)_{1+2x}(\text{PO}_4)_{5-2x}(\text{OH})$	Ca/P molar ratio 1.4 to 1.5
7. $\text{Ca}_{9+y}(\text{PO}_4)_{5+y+z}(\text{HPO}_4)_{1-y-z}(\text{OH})_{1-y+z}$	-
8. $\text{Ca}_{10-x+u}(\text{PO}_4)_{6-x}(\text{HPO}_4)_x(\text{OH})_{2-x+u}$	$2-x+2u \leq 2$ and $0 \leq u \leq x/2$

It is known that there are two types of apatite: biological apatite and apatite from mineral deposit. Biological apatite usually can be found in enamel, bone and dentin (Park, 2008). Synthesized apatite or often termed as “hydroxyapatite” is an effort to mimic biological apatite in the laboratory. The properties of HAP such as solubility and thermal stability are determined from the variation of their Ca/P molar ratio (Mostafa, 2005; Aizawa et al., 2006).

2.2.2 Substituted Hydroxyapatite

Besides stoichiometric HAP, there are many types of HAP which are known as substituted HAP (LeGeros and LeGeros, 2008). The HAP crystal is able to accept some impurities in its lattice such as CO_3^{2-} , F^- , Cl^- etc (Vallet-Regi and Gonzalez-Calbet, 2004). The substitution of HAP is achieved by partial replacement of the calcium (Ca^{2+}), phosphate (PO_4^{3-}), or hydroxyl (OH^-) ions in its crystal. This substitution yields various types of substituted HAP such as carbonated HAP, HAP containing fluoride, magnesium, strontium, etc (LeGeros and LeGeros, 2008). Carbonated HAP (C-HAP) is one of the substituted HAP products that have been

extensively studied due to its similarity with natural bone and its excellent properties over HAP (Landi et al., 2004; Fleet, 2009; Maruta et al., 2011).

2.3 Carbonated Hydroxyapatite

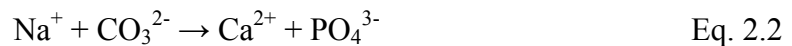
2.3.1 General Overview

Carbonated hydroxyapatite (C-HAP) has close chemical composition with the natural bone mineral (Landi et al., 2003). Considering the hydroxyapatite structure, carbonate (CO_3^{2-}) ions can substitute either the phosphate (PO_4^{3-}) ions or the hydroxyl (OH^-) ions of HAP, producing either a B-type or A-type C-HAP respectively (LeGeros et al., 1969). However, it is also possible for the CO_3^{2-} ions to substitute both of the PO_4^{3-} ions and OH^- ions, as reported by Rey et al. (1989), to form a AB-type C-HAP.

A-type C-HAP can be prepared by exposing a HAP sample in CO_2 environment at 900°C for 3 days. The formation of A-type C-HAP is presented in Eq. 2.1.



Preparation of B-type C-HAP is more complicated due to the charge imbalance (Gibson and Bonfield, 2002). However, it can be done by introducing sodium carbonate as the CO_3^{2-} ion source as well as sodium ions as the charge balance. This Na^+ ion is co-substituted by Ca^{2+} as presented in Eq. 2.2.



Another method to prepare a B-type C-HAP had been attempted by Zhou et al. (2008) without any co-substitution involved in the Ca^{2+} site. However, the results

suggested that C-HAP is calcium deficient with Ca/P molar ratio less than 1.67. AB-type C-HAP can be prepared as suggested by Gibson and Bonfield (2002) with a combination between wet reaction and sintering under CO₂ gas atmosphere.

2.3.2 Carbonated Hydroxyapatite as Bone Substitute

Carbonated hydroxyapatite (C-HAP) has been accepted as the ideal candidate for bone substitute material. It is due to the compositional similarity of C-HAP with natural bone mineral. Natural bone mineral is composed of HAP crystal with some impurities mainly carbonate (CO₃²⁻) ions as seen in Table 2.3 (LeGeros and LeGeros, 1993). Moreover, C-HAP is also believed to show better bioactivity since it possesses higher solubility compared to HAP (Ito et al., 1997). Various forms of C-HAP product have been produced for bone substitute purpose such as powder (Landi et al., 2003), dense (Daitou et al., 2010), and porous C-HAP (Wakae et al., 2008) forms.

Previously, hydroxyapatite (HAP) had been reported to be hardly resorbed by osteoclasts (Doi et al., 1999). If HAP cannot be resorbed by osteoclasts, new bone formation will not be formed (Wakae et al., 2008). It was reported that small amount of the CO₃²⁻ ions in HAP structure is able to increase its solubility significantly (Ito et al., 1997). Ito et al. (1997) further reported that the incorporation of one CO₃²⁻ ion per unit cell in HAP increased the solubility product by 10^{15.9} and 10^{11.0} for A-type and B-type respectively. The CO₃²⁻ content had also been proven to influence the amount of the viable cells attached and growth on the tested samples (Pieters et al., 2010). Hence, C-HAP has been considered as an ideal material for bone substitute.

Table 2.3 Component of Adult Human Bone (LeGeros and LeGeros, 1993)

Component	Bone (weight %)
Calcium, Ca^{2+}	24.5
Phosphorus, P	11.5
Carbonate, CO_3^{2-}	5.8
Magnesium, Mg^{2+}	0.55
Sodium, Na^+	0.7
Chloride, Cl^-	0.10
Potassium, K^+	0.03
Fluoride, F^-	0.02
Total inorganic	65.0
Total organic	25.0
Absorbed H_2O	9.7

2.4 Porous Carbonated Hydroxyapatite as an Ideal Bone Substitute

According to Stevens et al. (2008), candidates for bone substitute materials must follow several criteria for the success of developing new bone tissue. Bone substitute materials must be integrated with the surrounding tissue and provide initial three dimensional (3D) framework for cells to be attached and proliferated to produce new bone tissue. In fact, in order to be able to integrate with surrounding tissue, bone substitute materials must structurally and morphologically mimic natural bone. Natural bone is composed of carbonated hydroxyapatite crystals deposited in an organic matrix mainly collagen (Karageorgiou and Kaplan, 2005). In order to provide a suitable framework, several requirements for an ideal bone substitute must be followed (Stevens et al., 2008). These requirements are as follows:

1. Biocompatibility

The term biocompatibility is defined as the ability of a material to perform with an appropriate host response in a specific application (Williams, 1989). Biocompatibility refers to the lack of toxicity where an implanted material does not harm the living body during implantation.

2. Closely similar to the natural bone

An ideal bone substitute must be closely similar to natural bone both compositionally and structurally. It has been accepted that natural bone consisted of mainly a porous structure and C-HAP as the main minerals (Wakae et al., 2008).

3. Porous structure with interconnected pore networks

Porous material is therefore required for designing an ideal bone substitute. Porous material allows new bone tissue ingrowths as well as tissue invasion through its interpore connectivity (Yoshikawa and Myoui, 2005).

4. Appropriate surface chemistry to promote cells attachment, differentiation, and proliferation

Porous C-HAP has been reported to be able to promote cells attachment, differentiation and proliferation to produce new bone tissue (Li et al., 2012). Therefore, porous C-HAP becomes an ideal candidate as a bone substitute material.

2.5 Sponge Template Method for Fabricating Porous Apatite Biomaterials

There are many techniques available to produce bone scaffolds such as salt leaching, sponge template, gel casting, etc (Park et al., 2009; Wakae et al., 2008; Sepulveda and Binner, 1999). However, most of the techniques available are only

able to produce a closed pore material which is not an ideal candidate for bone substitute where interpore connection is required. Among them, sponge template method is the most popular technique to produce interconnected porous scaffold. This technique is the first method to produce macroporous ceramic by using a highly porous polymeric sponge typically polyurethane.

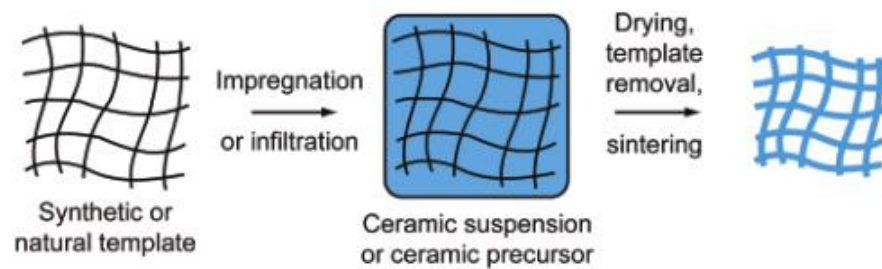


Fig. 2.2 Processing route to produce macroporous ceramics (Studart et al., 2006)

As previously mentioned, the sponge template that is usually used in this method is polyurethane (PU) foam. As a template, PU foam will be removed from the specimen during the sintering process to obtain the end product. The porous structure obtained from this method is actually the replication of the PU foam. Therefore, the porous structure obtained from this method depends on the morphology of the PU foam template (Fig. 2.2). Dressler (2009) had clearly explained the mechanism of how PU foam was removed from the coated slurry during sintering. Initially, the slurry is coated on the PU foam template. When the PU foam and slurry was sintered, gradually PU foam was removed from the slurry, remaining the empty space called hollow strut that is observed in SEM image as shown in Fig. 2.3. The mechanism of how the hollow strut is obtained is shown in Fig. 2.4. After heating to 260°C, most of the PU has been removed from the slurry. The residues that still remain in the slurry are totally removed after heating to 600°C.

The hollow strut then shrinks due to sintering. The same result was also reported by Studart (2006). A hollow strut was observed after the PU foam had been removed.

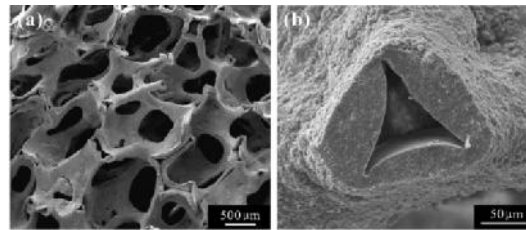


Fig. 2.3 SEM image after PU had been removed (Zhao et al., 2008)

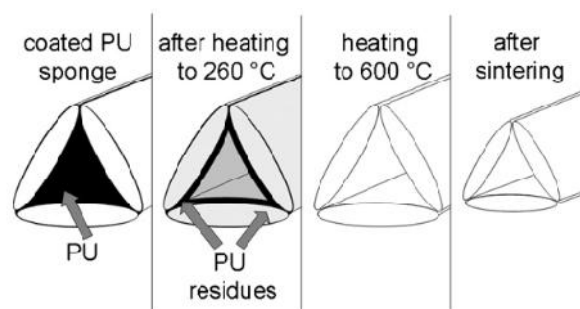


Fig. 2.4 Schematic illustration of the PU foam removal mechanism (Dressler et al., 2009)

The sponge template method allows the possibility to fabricate porous materials with pore sizes in the range of 200-500 μ m (Bellucci et al., 2011). Moreover, the sponge template method had also been reported to be able to produce porous materials with high porosity (Wakae et al., 2008). The pore size of porous materials for bone substitute is closely related with bone ingrowth. It was reported that pore sizes that were greater than 300 μ m have greater penetration of mineralized tissue in comparison with smaller pore sizes (Jones et al., 2004). The pores had significant effect on the formation of new bone tissue as shown in Table 2.1. Jones et al. (2004) also reported that the optimum pore sizes for bone ingrowth was in the range of 100-350 μ m.

The sponge template method requires sintering at relatively high temperatures to remove the PU foam and to provide strength to the porous body. In order to obtain the final porous product, however, the firing must be carefully done. Otherwise, the final product is a collapsed material instead of a porous material. Sufficient time and slow heating rate was required to remove PU foam without collapse (Li et al., 2002; Ramai and Zhang, 2003). Wakae et al. (2008) used two stages of sintering schedule to remove and sinter an α -TCP foam obtained by the sponge template method. during the first stage, a slow heating rate was scheduled to burn out the PU foam. At this stage, a soaking time might be added if necessary to provide sufficient time for PU foam to be completely removed before proceeding to the second stage to sinter the α -TCP foam.

2.6 Porous Apatite Biomaterials from Nano-sized Hydroxyapatite Powders

Nano-sized HAP powders have been reported for their remarkable biocompatibility (Huang et al., 2004). Smith et al. (2006) reported that porous HAP obtained from HAP nanoparticles (20nm) showed greater number of osteoblasts cells after seeding for 5 days compared with the one obtained from HAP coarse particle (10 μ m), whilst osteoblasts attachment did not show any difference. Smith et al. (2006) further showed that the use of HAP nanoparticles resulted in a smaller grain size (588 \pm 55 nm) compared with the one obtained from using coarser particles (8.6 \pm 1.9 μ m) as indicated in Fig. 2.5. Reduction in grain size then leads to an increase in grain boundary surface area that may improve some properties of the obtained porous product.

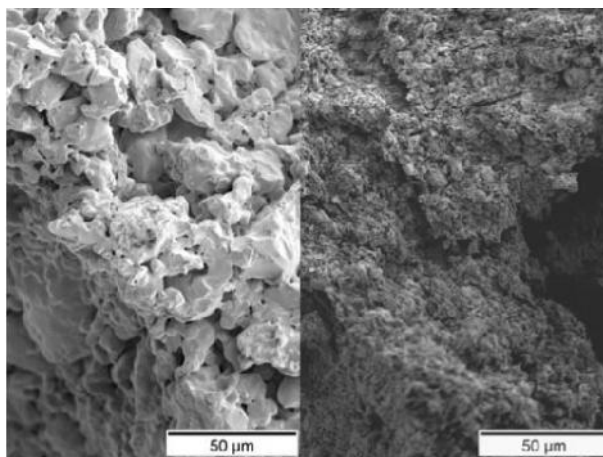


Fig. 2.5 Comparison of SEM images of the surface of scaffolds fabricated using HAP coarse particles (left) and HA nanoparticles (right) (Smith et al., 2006).

Besides, it was also reported that a porous HAP from nano-sized HAP powders could be sintered at a lower temperature and shorter soaking time (1100°C, 1h) compared to a porous HAP from micron-sized HAP powders (sintered at 1360°C for 4h) (Smith et al., 2006). However, there is no explanation given about the differences on the sintering temperature and soaking time used in the report. It may be due to the sinterability of nano-sized HAP powders which is higher than that of micron-sized HAP powders caused by larger surface area, thus reduced the sintering temperature (Yeong et al., 1999).

2.7 Methods for the Synthesis of Nano-sized HAP Powders

2.7.1 Hydrothermal Treatment

Hydrothermal is a term that originally came from the earth science which means regime of high temperatures and water vapor pressures (Sōmiya and Roy, 2000). This method is performed in an apparatus consisting of a steel pressure vessel called autoclave. The method has been known to be able to produce fine powders. The characteristic of hydrothermal powder is shown in Table 2.4. Besides,

hydrothermal method has benefits such as easy to control nucleation, high dispersion, high reaction rate, shape control, phase purity and homogeneity as well as cost effectiveness (Yoshimura and Byrappa, 2008).

Table 2.4 Characteristic of hydrothermal powder and ideal powder (Sōmiya and Roy 2000)

Parameters	Hydrothermal powder	Ideal powder
1. Grain size	Fine grain less than 1 μm	Fine powder less than 1 μm
2. Agglomeration	No or weak	Soft or no agglomeration
3. Particles size distribution	Narrow	Narrow
4. Homogeneity	Good	Good
5. Sinterability	Good	Good

Hydroxyapatite powder can be synthesized by hydrothermal treatment (Yoshimura et al., 1994). Yoshimura et al. (1994) reported that HAP whisker had been successfully synthesized from β-TCP in a water solvent with citric acid as the chelating agent by using a hydrothermal method. The powder obtained from this treatment was HAP with a Ca/P molar ratio of 1.63 which is slightly below the stoichiometric HAP (Ca/P=1.67). In addition, monetite (CaHPO₄) was also produced during the treatment. Moreover, Goto et al. (2012) reported that HAP fiber with a width size of around 130 nm was formed, which is in nanosize according to Gosh et al. (2004). Rod-like shape is the typical morphology of HAP obtained by a hydrothermal method (Yoshimura et al., 1994; Ioku et al., 2006; Earl et al., 2006; and Parthiban et al., 2011). The reaction mechanism of the HAP formation from β-TCP is shown in Eq. 2.3 (Parthiban et al., 2011).

